THEORETICAL AND EXPERIMENTAL INVESTIGATION OF SOME GENERAL SUSPENDED STRIPLINE DISCONTINUITIES

C. AMRANI*, M. DRISSI*, V. FOUAD HANNA** and J. CITERNE*

* URA CNRS 834, INSA DE RENNES, 35043 RENNES CEDEX

** CNET/PAB/STS, 92131 ISSY LES MOULINEAUX, FRANCE

ABSTRACT :

An integral equations technique associated with a 2D moment method, is used to characterise some general suspended stripline discontinuities namely : a stub, a meander, a bend and a bent-stub, for which two components for strip surface current are taken into consideration. A numerical simulation of a matched load at terminations of the studied discontinuities is achieved and is used for a precise determination of scattering matrix parameters for these discontinuities. Good agreement is achieved between numerical results and experimental ones that are obtained using the de-embeding calibration technique. The effect of parasitic waveguide modes is also discussed.

INTRODUCTION :

In spite of the several advantages that suspended stripline offers, namely : low losses and low dispersion characteristics, a comparative lack of CAD facilities especially for line discontinuities, is noticed. The problem was previousely treated either using a quasi static method [1]-[2] or using a dynamic analysis limited to the characterisation of uniaxial discontinuities [3]. So, the analysis given in this paper represents an effort toward the characterization of circuits realized in this very promissing technology, especialy at millimeter wavelengths.

The analysis is based on the use of the integral equations technique solved by a 2D method of moments. A simulation of a matched load [4] is then used for characterising both symmetrical and asymmetrical discontinuities. The theoretical results obtained by the present method are verified by experimental measurement using the de-embeding calibration technique.

ANALYTICAL FORMULATION :

The theory is based on the resolution of integral equations expressing the equality of the diffracted $\vec{E}^d$ and the feeding $\vec{E}^e$ electric fields on a conducting interface which can be written in the form :

$$\vec{e}_n \times \left[\vec{E}^d + \vec{E}^e\right] = \vec{e}_n \times Z_s . \vec{J}_s$$

where :
$\vec{e}_n$ is the unit normal vector.
Z_s is the conductor surface impedance
$\vec{J}_s$ is the surface current density

The diffracted electric field can be derived from vector and scalar potentials which are in turn expressed by electric GREEN's functions. Then, the surface current densities are obtained by the use of the method of moments through the 2D discritization of strip surface current which is expressed in terms of suitable basis functions :

$$\begin{bmatrix} Z^{xx} & Z^{xy} \\ Z^{yx} & Z^{yy} \end{bmatrix} \begin{bmatrix} I^x \\ I^y \end{bmatrix} = \begin{bmatrix} V^x \\ V^y \end{bmatrix}$$

where :
Z^{uv} (u,v=x,y) are submatrix elements.
I^u are current coefficients, and V^u are the coefficients of the exitation vector.

It is to be noticed that only the submatrix Z^{xx} has to be calculated when a 1D Moment method is used. For the present analysis, the whole submatrix elements are to be computed. Of course this is associated by an increase in the computing time. In closed structures, the GREEN's functions have not the same symmetry propreties, (which reduce the number of elements in each submatrix) like those for open structures . However, by using a rectangular sheet in the center of transverse plane (in both directions : ox and oy), many symmetry propreties can appear as : symmetry with respect to the center point and also with respect to ox and oy axes. This leads to considrable reduction in the required computational time. Moreover, the impedance matrix of many irregular discontinuites such as bends, stubs, bent-stubs or meander lines can be easily achieved from the correct combination of these 2D discretization.

The second step in this analysis is the extraction of the scattering matrix for both symmetrical and asymmetrical discontinuities Here a virtual matched load simulation is proposed [4]. The scattering parameters are then accurately determined from the numerical determination of the reflection ceofficient on the studied port when other junction ports are terminated by matched loads.

This technique has the advantage of being valid for the extraction of the [S] parameters not only for symmetrical discontinuities but also for asymmetrical ones.

NUMERICAL AND EXPERIMENTAL RESULTS :

The formulation described above was used to analyze some typical discontinuities. The results for a shielded bend discontinuity are given in figure 2 and are compared with those published in [5]. A good agreement is observed except around 15.5 GHz frequency which is the cut-off frequency of the higher order waveguide mode. In Figure 3, the magnitude and phase for S_{21} of a stub resonator are compared to measured values. The comparison shows a good agreement. One difficulty occurs when realizing a stub resonator at low frequencies is the appearance of higher order waveguide modes. This difficulty can be avoided by the use of a bent-stub. Figure 4 shows the variation of the magnitude of S_{11} as a function of frequency for a bent-stub resonator. In Figure 5 we present the variation of the magnitude of S_{11} for a meander discontinuity as a function of frequency for two positions of the meander circuit with respect to box vertical walls. It is observed that for an increasing offset, each of the resonance frequency and magnitude of S11 decreases. It is noticed that stub, meander and bent-stub discontinuities are realised on Duroid substrates (ε_r=2.22 and h=0.254mm) which are inserted in a WR28 waveguides. The experimental measurements were performed using the de-embeding calibration technique.

CONCLUSION:

A 2D moment method was used to analyse some general suspended stripline discontinuities. The variety of analysed discontinuities (bend, meander, bent-stub and astub) shows the perfect capacity of the present analysis to characterize any Nport planar discontinuity which can be represented by rectangular cells. The required computionnal time is not excessive compared to that required by other general numerical methods. A de-embeding technique of measurement has proven the validity and precision of our theoretical model. It is shown that the packaging has a considerable effect on the characteristics of the studied discontinuities.

REFERENCES :

[1] A. Rong, S.F. Li " Frequency Dependent Characteristics of Gap Discontinuities in suspended striplines for millimeter-wave applications" IEEE MTT-S Int. Microwave Symp.Digest, pp.355-358, June 1988.

[2] I.J Smith, "The even and odd mode capacitance parameters for coupled lines in suspended substrate" IEEE trans Microwave theory Tech., vol MTT-19, pp. 424-431, 1971.

[3] Achkar, O. Picon, V. Fouad Hanna, J. Citerne "Analysis of symetric and asymetric coupled suspended striplines and some associated discontinuites" 20th EuMC, pp.537-542, Sept. 1990.

[4] C. Amrani, M. Drissi, V.F. Hanna and J. Citerne, "An Electromagnetic Analyser for Suspended stripline Discontinuities" The 3rd ASIA-PACIFIC Microwave Conference Proceeding, pp. 431-434, Tokyo, 1990.

[5] A. Hill and V.K. tripathi, "An efficient algorithm for the three-dimensionnal analysis of passive microstrip components and discontinuities for microwave and millimeter-wave integrated circuits " IEEE trans Microwave theory Tech., vol MTT-39, pp. 83-91, Jan. 1991.

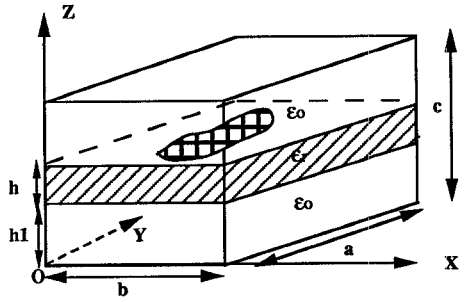

Figure 1-a : suspended stripline structure

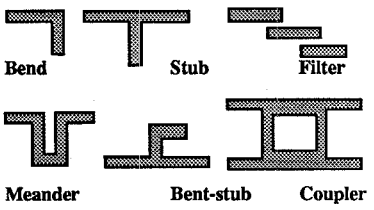

Figure 1-b : Some general suspended stripline discontinuities .

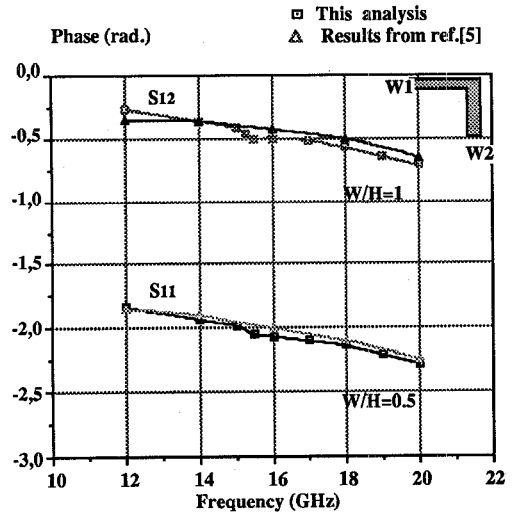

Figure 2-a

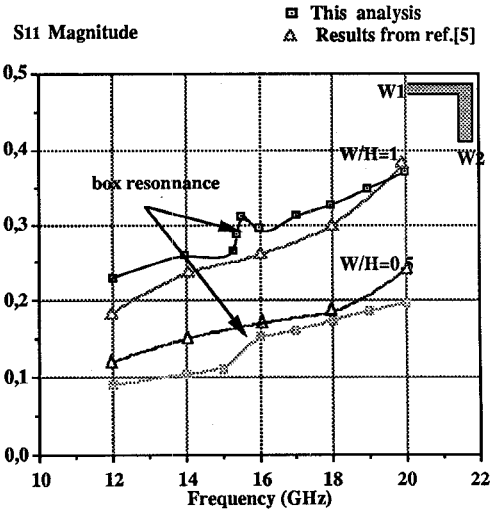

Figure 2-b

Figure 2 : The variation of S parameters of a bend discontinuity as a function of frequency, (W1=W2=W, a=b=12.7mm, h1=0mm, c=3.81mm, εr=9.8, h=.635mm)

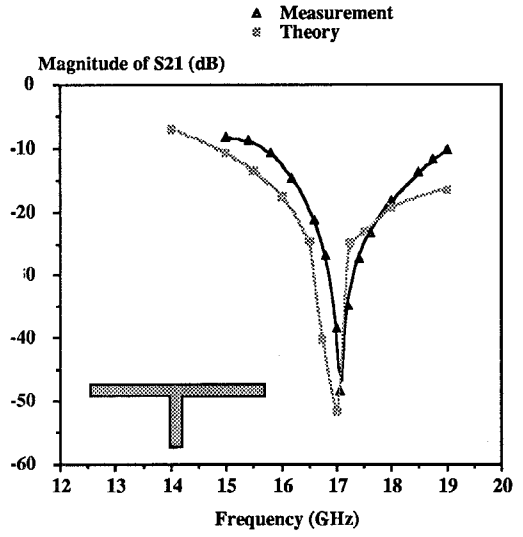

Figure 3-a : Variation of the S21 parameter magnitude as a function of frequency for a stub discontinuity.

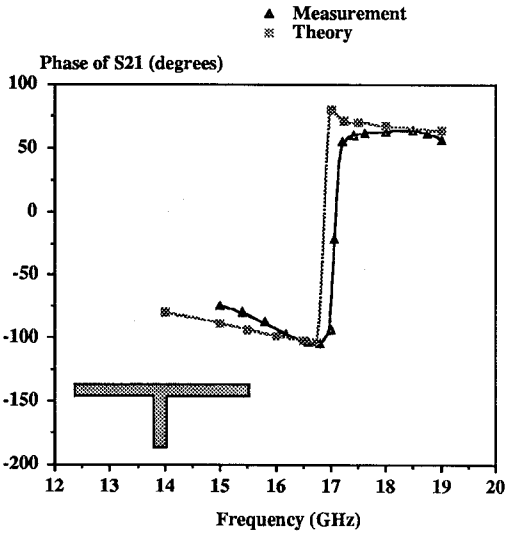

Figure 3-b : Variation of the S21 parameter phase as a function of frequency for a stub discontinuity.

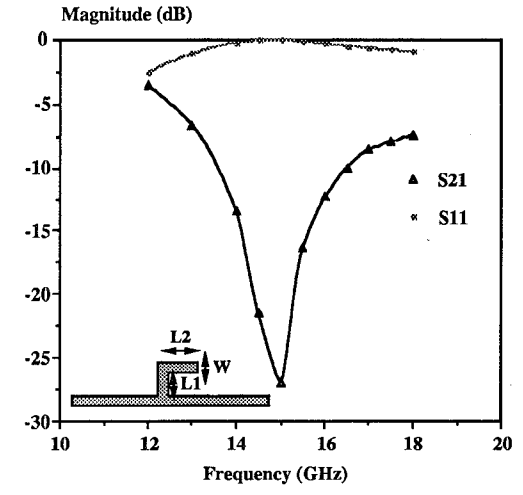

Figure 4 : Variation of S21 (dB) for a bent-stub discontinuity as a function of frequency. (L1= 2.358mm, L2=1.572mm, W=0.786mm)

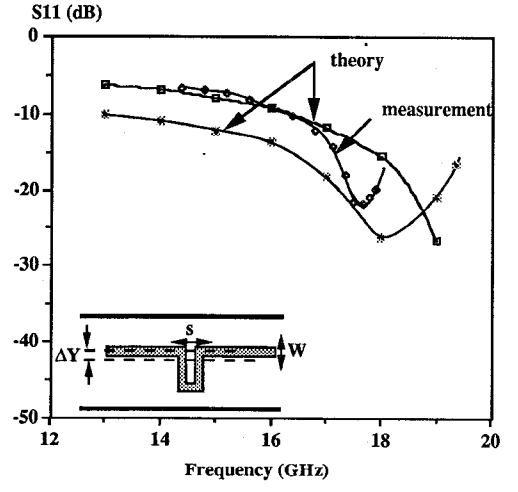

Figure 5 : Variation of the magnitude of S11 as a function of frequency for two meander positions . (W=0.786, S=W) :

- ΔY= 0 (theory)
- ΔY=.25mm (measurement)
- ΔY=.25mm (theory)